THE PENNSYLVANIA STATE UNIVERSITY
SCHREYER HONORS COLLEGE

DEPARTMENT OF BIOLOGY

Mitochondrial Dynamics In *Crithidia Fasciculata* And *Trypanosoma Brucei*

MADELINE F MALFARA
SPRING 2019

A thesis
submitted in partial fulfillment
of the requirements
for a baccalaureate degree
in Biology
with honors in Biology

Reviewed and approved* by the following:

Megan Povelones
Assistant Professor of Biology
Thesis Supervisor

Elizabeth Dudkin
Associate Professor of Biology
Faculty Reader

Hans Schmidt
Assistant Professor of Communications
Honors Adviser

* Signatures are on file in the Schreyer Honors College.

ABSTRACT

Trypanosoma brucei and *Crithidia fasciculata* are model organisms for studying mitochondrial dynamics. Since these organisms diverged early in eukaryotic history, they offer insights into important processes that have been conserved throughout the eukaryotic lineage. *T. brucei* have well-developed techniques for studying the function of genes, such as RNA interference (RNAi). *C. fasciculata* are another useful model for mitochondrial dynamics; however, there are not yet well-established genetic techniques to investigate the role of different genes. We have created and validated mitochondrial-GFP (mitoGFP)-expressing *T. brucei* and *C. fasciculata* cell lines. With this construct, we have performed RNAi in *T. brucei* to confirm some of the published phenotypes of dynamin-like-protein (DLP). We have also created a CRISPR/Cas9 *C. fasciculata* cell line, which can be used to knockdown many different proteins, including DLP. After confirming the expression of the CRISPR/Cas9 plasmid, we plan to knockdown *pf16*, a central axoneme protein of the flagellum, to show that we can use this system to rapidly study gene function in *C. fasciculata.* We also plan to fuse a destabilizing domain construct to DLP in *C. fasciculata*, in order to study the role of, what is likely an essential, protein.

TABLE OF CONTENTS

LIST OF FIGURES

LIST OF TABLES

No table of figures entries found.

ACKNOWLEDGEMENTS

Start here or [Insert]/(File) here ...

Chapter 1

Introduction

Dynamin-like proteins (DLPs), also known as dynamin related proteins (DRPs), help to mediate mitochondrial division and fusion events through GTPase activity (Lackner, 2013). They differ from classical dynamins in that they lack the Plekstrin homology (PH) domain and proline-rich domain (Hinshaw, 2000). The PH domain helps recruit dynamin to the membrane. The absence of a PH domain in DLP suggests that adaptor proteins may be present to help recruit DLP to the membrane. DLPs are thought to be involved in many different functions, but are most often involved in changing of membrane morphology (Hinshaw, 2000). While DLP is well studied in some organisms, such as *Saccharomyces cerevisiae*, much is unknown about it in other organisms, and it remains a protein of interest to researchers studying kinetoplastids.

Kinetoplastids are single-celled eukaryotes that are set apart from other eukaryotes by the formation of a kinetoplast. The kinetoplast is a structure that holds all of the mitochondrial DNA (kDNA). We study a subset of kinetoplastids, known as trypanosomatids, which are flagellated and parasitic in nature. We specifically study *Trypanosoma brucei* and *Crithidia fasciculata. T. brucei* are a human infective species of parasite, and are the causative agent of human African trypanosomiasis, or African Sleeping Sickness. *T. brucei* exist as bloodstream form (BSF) in the mammalian bloodstream and as procyclic form (PCF) in the midgut of their vector, the tsetse fly. We are able to culture both PCF and BSF *T. brucei* in the laboratory.

Both BSF and PCF are always extracellular, which is to say that they never invade the host or vector cells, rather they remain in the bloodstream at all times. This is especially unusual

for a parasite that infects mammals since antibody-mediated immunity is so robust. High concentrations of glucose in the mammalian bloodstream creates a nice environment for *Trypanosomes*. Because of high levels of glucose, BSF are able to make ATP through glycolysis, rather than through oxidative phosphorylation, which is the main source of ATP in PCF. For this reason, BSF have a simpler mitochondrial network with few cristae. Although the mitochondrion is not being used to make energy in BSF, it is still required for other essential functions, like synthesizing fatty acids and regulating metabolic pathways. On the other hand, PCF require a very active mitochondrion, since they metabolize amino acids for energy. For this reason, they have a highly branched mitochondrial network with lots of cristae.

Another related organism, *Crithidia fasciculata*, is a kinetoplastid with only one host—the mosquito. *C. fasciculata* are good models for studying mitochondrial dynamics since they are easy to grow in large quantities, and are genetically very similar to other kinetoplastids, but only have one host. *Crithidia* also diverged very early in the evolutionary lineage of eukaryotes, so they are a good model for understanding the basal components of mitochondrial machinery. Like all kinetoplastids, they only have one mitochondrion per cell. Most eukaryotes have many mitochondria per cell, which makes them difficult to study. The single mitochondrion of kinetoplastid parasites makes the synchronization of mitochondrial biogenesis and division with the cell cycle especially important. One problem with using *C. fasciculata* as a model, is the lack of rapid and effective means of genetic manipulation. However, since the genome sequence has been released, the development of these technologies within *Crithidia* is possible. Before investigating the role of DLP in kinetoplastids, first the structure of the cell should be examined, specifically the mitochondrion.

The biogenesis, positioning, and segregation of the mitochondria are crucial to cell survival. Kinetoplastids have a complex known as the tripartite attachment complex (TAC), which connects the basal body to the kDNA (Hoffmann, 2018). Hoffmann et al. propose a novel model for mitochondrial segregation in *T. brucei*. Through superresolution microscopy they were able to identify the location of all of the parts of the TAC that are currently known, and determine that it is likely assembled in a hierarchal order, starting at the base of the flagellum and building towards the kDNA. Hoffmann et al. most notably discovered that the TAC is needed to position the mitochondrion correctly, but is not needed for the biogenesis or segregation of the mitochondria. While correct mitochondrial positioning is crucial to cell health, another cell component that should be considered is actin.

Actin is a well-characterized cytoskeletal element in higher eukaryotes, but the function of actin in *Trypanosomes* has been unknown up until recently. García-Salcedo et al. found that actin is required for proper endocytosis in BSF *T. brucei* (2004). They used tetracycline induced RNAi of actin in BSF *T. brucei*. Depleting actin caused the rapid arrest of cell division, the halting of vesicle movement from the flagellar pocket to the membrane, the stopping of endocytic activity, and cell death. This “big-eye” phenotype, where the flagellar pocket swells, is a well-defined phenotype that indicates problems with the endocytic pathway, since all endo- and exocytosis occur at the flagellar pocket. There are many ways to investigate the role of a protein in a cell, and when available a chemical inhibitor is an easy and efficient way to explore a protein’s function.

Previously, there were few known chemical inhibitors of dynamin. Cassidy-Stone et al. performed a large-scale chemical screen to find inhibitors of mitochondrial division (2008). Classical dynamins that are involved in mitochondrial division directly regulate the

permeabilization of the outer mitochondrial membrane, which is a separate event from Drp1-mediated division (Cassidy-Stone, 2008). Cassidy-Stone et al. found a chemical inhibitor of mitochondrial division, which they named mdivi-1. This inhibitor was found to selectively inhibit dynamins involved in mitochondrial division in both yeast and mammalian cells. They hypothesized that mdivi-1 works by preventing apoptosis through inhibiting the permeabilization of the outer mitochondrial membrane. Specifically, they believe that mdivi-1 prevents cytochrome c release from mitochondria. It is likely that mdivi-1 functions similarly in kinetoplastids such as *C. fasciculata* and *T. brucei*, and could be used to study the role of DLP in those cells.

While findings have been published on the role of DLP in *Trypanosoma brucei*, there has yet to be a comprehensive review on the topic. DLP has been shown to localize to the mitochondria (Morgan et al., 2004) and to be important in endocytosis (Chanez et al., 2006), but there are still questions as to if DLP plays a role in regulation of the cell cycle. The function of DLP in *Crithidia fasciculata* has yet to be observed, to our knowledge.

The kinetoplastid genomes are missing a number of mitochondrial dynamic homologs found in higher-level eukaryotes. Only a few homologs have been identified bioinformatically, and while some have been well characterized, many have yet to be investigated. In *T. brucei*, the protein TbDLP has been identified as a homolog to the human protein dynamin-related protein 1 (DRP1). Humans have both classical dynamins, which are responsible for the division of vesicles in clathrin-mediated endocytosis, and dynamin-like proteins, which are involved in membrane fission. However, kinetoplastids lack classical dynamins, and only have dynamin-like proteins (DLP) or dynamin-related proteins (DRP). Dynamin-like proteins are made up of an N-terminal GTPase domain, a middle stalk domain, and a C-terminal GTPase effector domain. They lack the

transmembrane domain, Plekstrin homology domain, and proline rich domain found in classical dynamins. Since they lack the Plekstrin homology domain, which is important in recruiting classical dynamins to the membrane, DLPs must require adaptor proteins to anchor the protein to the membrane. However, adaptor proteins in *T. brucei* have yet to be identified. Currently there is some debate over the role of DLP in kinetoplastids.

While some research has shown that DLP is involved in both mitochondrial division and endocytosis, work by other groups did not find evidence for a role for TbDLP in the endocytic pathway. The first publication on TbDLP (Morgan et al.) stated that *T. brucei* have one DLP, TbDLP, and that this feature is conserved across kinetoplastids (2004). More recent studies have challenged the idea that there is one DLP, and instead have argued that there are 2 DLP paralogs. Morgan et al. also showed colocalization of TbDLP to the mitochondrion. RNAi depletion of TbDLP caused mitochondrial morphological changes, but did not affect the structure of other membrane-bound compartments, like those responsible for the endocytic and exocytic pathways. The DLP-depleted cells also had a collapsed or fused mitochondrial network, and an accumulation of membrane constriction sites, as seen by electron microscopy. Morgan et al.'s 2004 study was the first to show DLP's involvement in the mitochondrion, but future studies found that DLP may be involved in other pathways as well.

Later, Chanez et al. found that DLP is needed for mitochondrial division, and that this event serves as a cell cycle checkpoint in the cell cycle of *T. brucei* (2006). Previously, Chanez et al. showed that expressing Human Bax, a proapoptotic protein, in *T. brucei* led to fragmentation of mitochondria. In this new study, Chanez et al. showed that depleting both Bax and DLP in the same cells did not result in mitochondrial fission. This indicates that DLP may be responsible for Bax-induced mitochondrial fission, and may therefore be required for proper

mitochondrial division during the cell cycle. DLP-depleted cells also had characteristic “big eye” phenotypes, indicating an endocytic defect. All endo- and exocytosis occurs at the flagellar pocket in *T. brucei.* So, when the flagellar pocket swells, it looks like an eye. In localization studies, they showed that DLP localizes to the mitochondrion and to the flagellar pocket. This is another indication that DLP has a dual role, in both endocytosis and mitochondrial fission. Chanez et al. also hypothesize that mitochondrial fission may become a checkpoint for cytokinesis, since DLP depletion resulted in multinucleated cells that had arrested before cytokinesis, which would not be caused by an endocytosis defect. Chanez et al. confirmed Morgan et al.’s findings that DLP is related to mitochondrial fission, but also discovered that DLP plays a role in the endocytic pathway and, possibly, regulation of the cell cycle. This difference in findings could be attributed to different knockdown efficiencies. It is possible that Morgan et al. only partially knocked down TbDLP, while Chanez et al. was able to knockdown TbDLP fully. Up until this point it was still thought that *Trypanosomes* only had one DLP.

A recent study by Benz et al. found that *T. brucei* have two paralogs of DLP, TbDLP1 and TbDLP2, which differ by only 19 amino acids (2017). This finding was surprising, since *Trypanosomes* are the only kinetoplastid analyzed so far that has more than one predicted DLP. When TbDLP1 was overexpressed, it was able to rescue the endocytosis and growth defect in BSF *Trypanosomes*; however, TbDLP2 was not able to rescue BSF cells. TbDLP1 is essential and sufficient for BSF, but PCF need both paralogs. The big eye endocytic defect phenotype, seen in Chanez’s experiments, was replicated in this study. However, the PCF cell lines did not show the cell cycle defect described in Chanez et al. While mitochondrial constrictions were observed, they did not see a complete absence of mitochondrial division. It was suggested that post-translational modifications could be responsible for the differing functions of the two

paralogs of TbDLP. Moreover, neither paralog of TbDLP could fulfill all functions necessary for normal cell growth. Both rescue lines had slowed growth compared to wild type cells, and growth was inhibited in RNAi induced lines. Benz et al. hypothesize that endocytosis may not be as important in PCF, so those cells were able to withstand a slight downregulation; however, BSF rely more heavily on endocytosis which led to more rapid cell death. Again, Morgan et al.'s mitochondrial phenotype was replicated, in addition to Chanez et al.'s endocytosis defect, but the cell cycle phenotype was not observed. In addition, unlike Morgan et al.'s experiments which found one DLP, Benz found two paralogs of TbDLP, with a division of roles for each. This could be attributed to improvements in the genome sequence.

The disagreement on the multiple roles of DLP in kinetoplastids, paired with the recent discovery of two paralogs of DLP in *T. brucei*, begs the questions, how much do we really know about DLP? First, a consensus must be reached on whether DLP is involved in endocytosis. It seems to be agreed upon that DLP plays a role in mitochondrial division. To further study DLP's role, depletion experiments ran by Morgan, Chanez, and Benz must be replicated. In addition, DLP should be studied in other kinetoplastids. For example, *Crithidia* only have one DLP, unlike *T. brucei*, who have two paralogs. This may be explained by the complex life cycle of *T. brucei.* Perhaps by studying DLP in *Crithidia*, we can elucidate the role of these two paralogs, or at least settle the endocytosis debate. RNA interference machinery has yet to be established in *Crithidia*, so a different method for studying DLP must be used, such as CRISPR.

Recently, Beneke created a CRISPR/Cas9 cell line in *Leishmania*, a closely-related kinetoplastid (Beneke, 2017). CRISPR is a genetic editing tool used to manipulate DNA. This cell line made it possible to knockdown or tag any gene of known sequence in the *Leishmania* genome. The creation of a CRISPR/Cas9 cell line in *Crithidia* would make it possible to study a

wide variety of genes, including DLP. We would be able to characterize DLP in *Crithidia*, and see how it relates to what has been published on the role of DLP in other kinetoplastids (i.e. Benz, Chanez, Morgan). CRISPR/Cas9-mediated cleavage would greatly increase the efficiency of homologous recombination, which will make gene knockout a more likely event. A potential problem with investigating the role of DLP is that it is thought to be essential. So, if we knock out DLP, it is possible that the cells will not be healthy enough to divide, and we would not be able select for transfectants.

Fulwiler et al. have found a potential solution to this essential gene problem: the introduction of a destabilizing domain (2011). A destabilizing domain fuses one copy of a gene to a domain, that in the presence of the ligand FK506, is stable. However, in its absence, the gene becomes destabilized and depleted. Fulwiler et al. employed the use of a four-way ligation to create a destabilizing domain both rapidly and efficiently. Normally, only two constructs are ligated together at one time. Accurate four-way ligations make the creation of knockout/in constructs much more efficient. Since *Leishmania*, *Trypanosomes*, and *Crithidia* are diploid, they have two copies of every gene. Therefore, one copy of DLP could be knocked out entirely, while the other copy continues to function normally. The copy that is not knocked out could then be fused to a destabilizing domain, so that in the presence of the ligand it would be stable and the cells could continue to grow normally. Then, to study DLP, you could remove the ligand to destabilize the protein and observe the effects. The ability to control the stability of DLP would allow for normal cell growth throughout the experiment. This could solve the problem of studying essential genes, such as DLP.

Combining Fulwiler's destabilizing domain with Beneke's CRISPR/Cas9 cell line, could lead to a useful tool for studying genes like DLP. A destabilizing domain construct for *Crithidia*

DLP could be created using Fulwiler's four-way ligation protocol. Then, the destabilizing domain construct could be introduced to the CRISPR/Cas9 *Crithidia* cell line, and the essential protein DLP could be inducibly knocked down in *Crithidia*.

There is still much controversy over the role of DLP in *Trypanosomes*. Everyone seems to agree that it is involved in mitochondrial division; however, there is still uncertainty as to if it is involved in endocytosis. Creating a CRISPR/Cas9 cell line in *Crithidia* would allow us to study many different mitochondrial dynamic proteins. Since DLP is the most well-characterized of the mitochondrial dynamic homologs known, and to our knowledge it has never been studied in *C. fasciculata*, it is a great first candidate to study.

Chapter 2

Materials and Methods

Cell culture

CfC1 strain *Crithidia fasciculata* were grown at 27°C on a rocker in brain heart infusion (BHI) medium supplemented with 20 μg/ml bovine hemin (Sigma). Selection drugs were added to the media as needed in the following concentrations: 30 μg/ml G418, 200 μg/ml hygromycin, and 60 μg/ml blasticidin. Cells were passaged every 2-3 days in order to keep them at a density between 10^6 and 10^8 cells/ml. Cell density was calculated by adding 25 μL of 3% formalin to 25 μL of cell culture and mixing, followed by adding 200 μL of crystal violet stain before loading the sample onto a hemocytometer to count. *Trypanosoma brucei* strain TbPCF 29-13 with mitoGFP was grown at 27 °C on a shelf in SDM-79 supplemented with 7.5 μg/ml bovine hemin (Sigma) and 10% fetal bovine serum (FBS). Selection drugs were added to the media as needed in the following concentrations: 15 μg/ml G418, 50 μg/ml hygromycin, 5 μg/ml blasticidin, 2.5 μg/ml phleomycin, and 1.0 μg/ml puromycin. Cells were passaged every 2-3 days in order to keep them at a density between 10^5 and 10^7 cells/ml. Cell density was calculated by loading sample onto hemocytometers and counting live.

Transfection

For *C. fasciculata*, 5 X 10^7 cells were spun down at 1000 rcf for 5 minutes for each sample, unless the sample was larger than 1.5 ml in which case it was spun at 1000 rcf for 10 minutes. Cell pellets

were resuspended in 100 μL supplemented Lonza Human T-cell nucleofector solution, followed by an addition of 19 μg of purified DNA, at a concentration of 0.5-2 μg/ml. Mock cells were resuspended in 100 μl BHI media. Cells were transfected using program X-001 in a Lonza Nucleofector II device, followed by recovery in 5 ml of media in a flask, without drug, overnight at 27°C on a rocker. After 24 hours cells were spun down as before and resuspended in 5 ml of media with selecting drug. For *T. brucei* 1 X 10^8 cells/ml were spun down and resuspended in 100 μL supplemented Lonza Human T-cell nucleofector solution. A mock sample was resuspended in SDM-79 medium. They were transfected using program X-014 in the Lonza Nucleofector II. Following transfections, cells were allowed to recover in the 5 ml media without drug for 18-24 hours, at which point they were spun and resuspended in fresh medium containing the appropriate amount of selecting drug. For *in vivo* sgRNA transcription, CfpTb007 cells were transfected with 4 μg of donor DNA (2 μg of each donor cassette) and 4 μg of sgRNA template DNA (2 μg of each sgRNA). The drug resistant transfectants came up between 1 to 2 weeks after resuspending in selecting drug.

CRISPR/Cas9 cloning strategy

The pTb007 plasmid, including genes for both the SpCas9 nuclease and the T7 polymerase, (a gift from Eva Gluenz, Beneke et al. 2017) was transfected into our CfC1 cell line, selected using hygromycin, and expressed as an episome. Expression of the FLAG-tagged Cas9 protein was confirmed by western blotting. As an alternative strategy we sought to integrate the Cas9/T7 construct into the beta-tubulin locus of *C. fasciculata.* The *Leishmania* upstream and downstream targeting signals were replaced with homology flanks corresponding to the beta tubulin intergenic region of *Crithidia fasciculata.* To do this, an intermediate construct was first created that could target GFP into the *C. fasciculata* tubulin intergenic region. A 4-way ligation protocol, as designed by Phillip Yates 2011, was employed to join the following fragments together: upstream of *Crithidia* beta tubulin, downstream of *Crithidia* beta tubulin,

pBB backbone, and the GFPHyg cassette from the pNUS vector. This construct was confirmed by diagnostic digest and sequencing and is referred to as pNUSbetatubGFPHygcH. This plasmid was digested**,** purified, and introduced into the wild-type Cf-C1 parental line by nucleofection. After selection with hygromycin, cytoplasmic GFP expression was confirmed by fluorescence microscopy. We are still working on cutting out the 5' beta tubulin targeting fragment and the upstream processing signal from the pNUSbetatubGFPHygcH to replace the Leishmania tubulin targeting sequence and upstream processing signal in pTb007. Similarly, we are still trying to replace the downstream tubulin targeting sequence and processing signal in pTb007 with that found in pNUSbetatubGFPHygcH**.**

Designing sgRNA

The sgRNA was designed as in Beneke et. al paper. The Eukaryotic Pathogen CRISPR guide RNA/DNA Design Tool (http://grna.ctegd.uga.edu) was used to choose guide RNA sequences with the following parameters: SpCas9: gRNA length 20; PAM: NGG; off-target PAM: NAG, NGA). Approximately 45 bp region upstream of the start of the coding region and 45 bp downstream of the stop codon of the gene of interest were used as the search query, with *C. fasciculata* chosen as the genome. A 20 nt guide RNA sequence was selected, regardless of if it was on the Watson or Crick strand. sgRNA's were chosen based off of close proximity to the coding region, and avoidance of areas with known SNP's. Primers were designed by adding the T7 promotor binding sequence to the guide from the Design Tool with the 3 nt PAM sequence removed, with the scaffold binding region at the end of the primer. The 3' donor DNA primers were made by adding the reverse complement of the 30 nt homology region to the universal primer for downstream of the drug cassette in the pTNeo plasmid. The 5' donor DNA primers were designed by adding the universal primer for upstream of the drug cassette in the pTNeo plasmid to the 30 nt homology region. The scaffold primer was used from G00 primer sequence found on http://leishgedit.net/.

Western blot

Cell lysates were made in 1 X SDS Page loading buffer. The samples were loaded on a 12% SDS-polyacrylamide gel and transferred to a polyvinylidene difluoride (PVTF) membrane. The membrane was incubated in 5% milk solution in 1X PBS to block overnight at 4 °C. The membrane was then probed in 1% milk solution with 1:10,000 dilution of mouse αFLAG antibody for 3-4 hours. The membrane was washed with PBST and then probed with goatαmouse HRP antibody for 1 hour, and incubated with ECL (BioRad). The gel was imaged with a G:Box gel imager, with 5 minutes as the longest exposure.

Microscopy

Both *C. fasciculata* and *T. brucei* cells were fixed prior to fluorescence microscopy. For *C. fasciculata,* 1 X 10^7 cells from a mid-log phase culture were harvested by centrifugation at 1000 rcf for 5 minutes, followed by resuspension in 1 ml BHI and addition of 36% formaldehyde solution to a final concentration of 4%. Cell were fixed at room temperature for 5 minutes, spun again, and washed 2X in 1 ml PBS. Cells were resuspended in 1 ml of PBS and 200 μL was applied to a charged slides (Thermo) for 10-20 minutes in a humid chamber. The slides were then washed in PBS before permeabilizing in PBS containing 0.1% Triton X-100, staining with 0.2 μg/ml DAPI, and mounting in 90% glycerol. For MitoTracker staining, cells were incubated at 27°C in pre-warmed BHI medium containing 5 μL of 1 mM MitoTracker Red CMXRos for 30 minutes. Cells were then centrifuged and resuspended in BHI without stain. Cells were incubated for 10 minutes at 27°C before fixation with formaldehyde and DAPI staining. Images were taken on a Zeiss Axiscope.A1 upright LED fluorescence microscope equipped with a Zeiss AxioCam ICm1 camera. Wide-field fluorescent images were taken in phase, GFP, RFP, and DAPI. For *T. brucei,* 1 ml of cells were prepared from a culture at ~1 X 10^7 cell/ml. Otherwise fixation conditions were

the same as for *C. fasciculata*, except when staining with MitoTracker, only a 20-minute incubation at room temperature was used.

RNAi/Overexpression

The *T. brucei* dynamin-like protein DLP RNAi construct, pALC15, and the DLP overexpression construct, pALC21, (a gift from Chanez et al.) were transfected into our mitoGFP *T. brucei* cell line, TbmitoGFP. The cells were cloned by limiting dilution using 0.4 cells/well. After the cells had recovered, RNAi was induced using 1 μL of 5 mg/ml doxycycline in 5ml culture. Overexpression was induced using 0.8 μL of 5 mg/ml doxycycline in 4 ml culture. Fluorescent microscopy and growth curves were performed on clones in triplicate.

Bioinformatics

TbDLP (Tb927.3.4720 and Tb927.3.4.4760), CfDLP (CFAC1_200029900), LdDLP (LdBPK_292310.1), LiDLP (LINF_290029700), LmjDLP (LMJLV39_290030000), LmnDLP (LmxM.08_29.2200), TcDLP (TcCLB.508153.20), LpDLP (LpyrH10_08_2620), PcDLP (PCON_0039990), TcDLP (TclL3000_0_42670), TeDLP (TevSTIB805.3.5000 and TevSTIB805.3.5040), and TvDLP (TvY486_0304114) sequences were retrieved from the TriTrypDB website (www.tritrypdb.org), ScDLP (NP_013100.1), DmDLP (CAA42067.1), CeDLP (NP_741403.2), HsDLP (AAC23724.1)DrDLP (NP_957216.1)XlDLP (NP_001079557.1), and TtDLP (ABB13595.1) sequences were retrieved from the NCBI website (https://www.ncbi.nlm.nih.gov) and were aligned using Clustal Omega. Domain diagrams were made in Microsoft PowerPoint and information within was obtained from the InterPro Website (http://www.ebi.ac.uk/interpro/search/sequence-search).

Kinetoplastid DLP homologs were identified and retrieved from the TriTrypDB website. The full dataset was then aligned in Clustal Omega and put into the PhyML website (http://www.atgc-montpellier.fr/phyml/) after removing gaps using Jalview. The Bayesian Information Criterion was used with 100 bootstrap replicates to create a phylogenetic tree.

Plasmid/Construct Formation

I need help writing this section. MitoGFP in *T. brucei*, pALC15, pNUS and pT plasmid modification. We had also talked about adding a table with primer sequences.

Chapter 3

Bioinformatics Analysis of DLP in Kinetoplastids

While DLP and classical dynamin share some characteristics, DLPs are missing some domains that are present in dynamin, have different ways of interacting with the membrane, and perform functions diverse from classical dynamins (Hinshaw, 2000). **Figure 1**. shows the domain structure for *T. brucei* DLP, *C. fasciculata* DLP, and both *H. sapiens* dynamin and DLP. Human classical dynamin, shown in

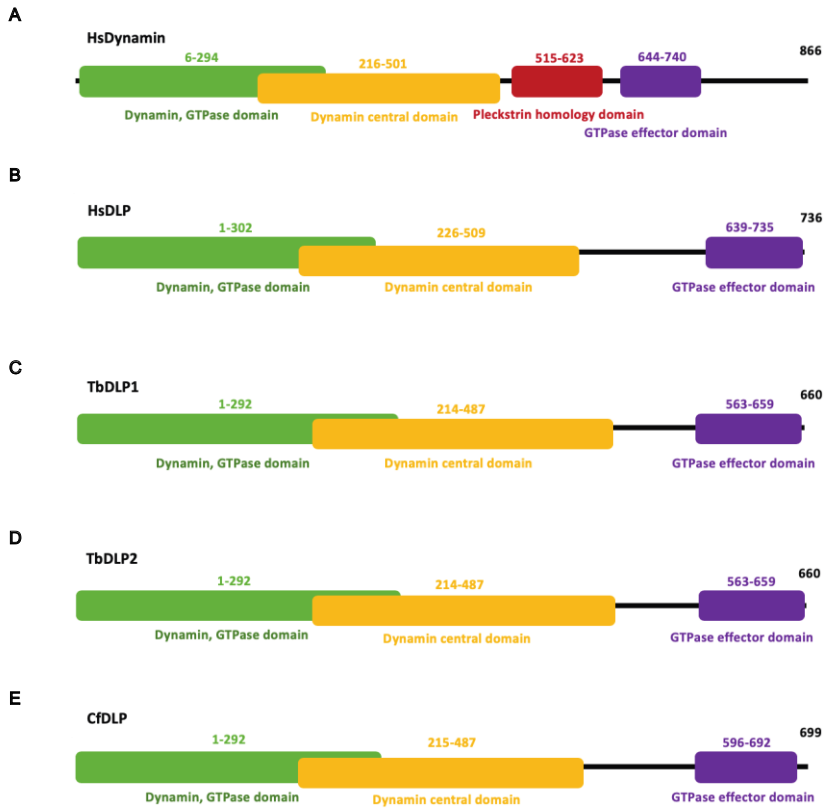

Figure 1. DLP and dynamin domain diagrams

Both paralogs of TbDLP have identical domain diagrams. This is expected since TbDLP1 and TbDLP2 differ by only 19 amino acids. CfDLP has a domain diagram very similar to TbDLP. All 3 have a GTPase domain, dynamin central domain, and GTPase effector domain. Classical dynamin, in this case *Homo sapiens*, also shares these 3 domains, but in addition has a Pleckstrin homology domain. It should be noted that *H. sapiens* DLP contains the same 3 domains as TbDLP and CfDLP, and lacks the PH domain.

Figure 1. A, has an extra domain, the Plekstrin homology (PH) domain. This PH domain allows dynamin to associate with the membrane. Since DLPs lack a PH domain, it is likely that adapter proteins are required to interact with the membrane and recruit DLP.

While many organisms have both dynamin and DLP, kinetoplastids lack classical dynamins, and only have DLP. DLPs are ancient in evolutionary origin, and are actually ancestral to classical dynamins (Ramachandran, 2018). This helps to explain why kinetoplastids only have DLPs and not dynamins, since kinetoplastids evolved earlier in the eukaryotic lineage.

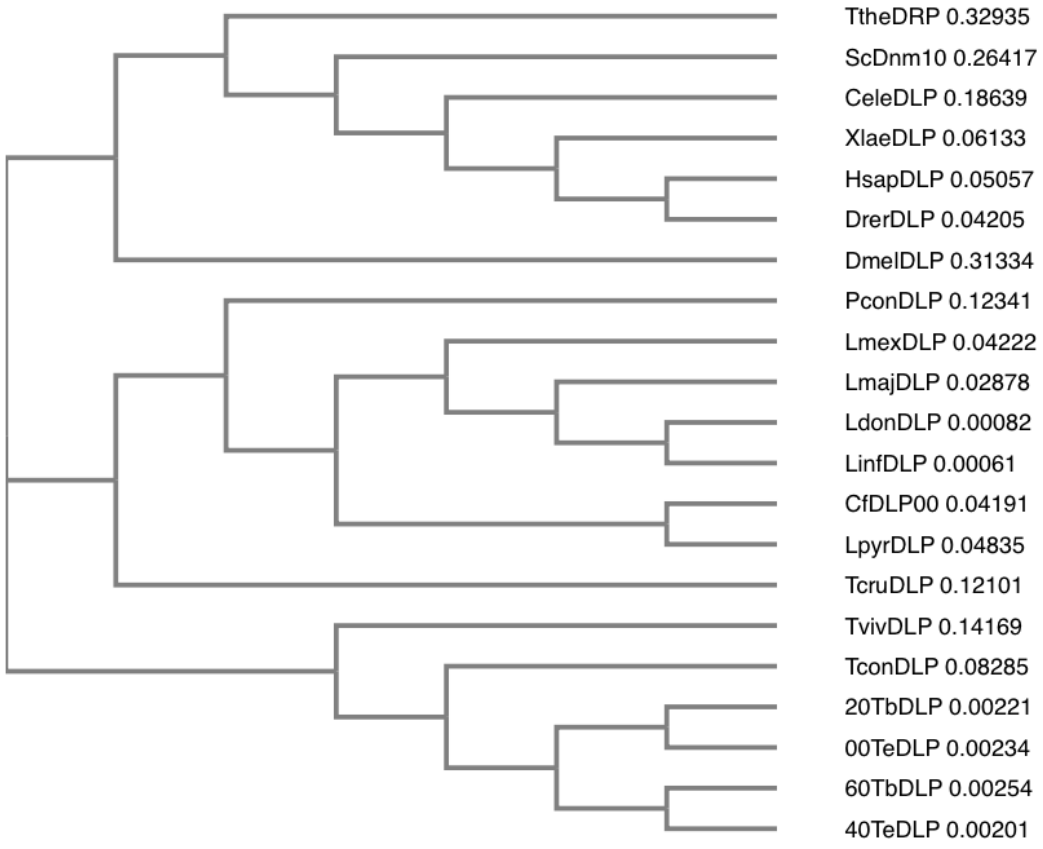

Figure 2. Clustal Omega Phylogenetic Tree of DLP Homologs

Phylogenetic tree from Clustal Omega of DLP homologs from various kinetoplastids and common model organisms. Interestingly, *T. evansi* have two paralogs of DLP that group with the *T. brucei* DLP paralogs. The kinetoplastids group together as well as later diverged eukaryotes.

In *H. sapiens*, DLP is only involved in mitochondrial functions; however, in kinetoplastids DLP may be involved in both mitochondrial dynamics and endocytosis (Chanez et al., 2006).

Almost all kinetoplastids have one DLP. *T. brucei* are the exception, as they have two closely-related paralogs of DLP, TbDLP1 and TbDLP2. Both paralogs are necessary, and while they seem to have some overlapping function, knockdown studies indicate that each paralog is performing a distinct function in the cell. It was previously thought that *T. brucei* was the only kinetoplastid to have two paralogs of TbDLP (Benz et al., 2017). However, our bioinformatic analysis revealed that the closely-related organisms, *Trypanosoma evansi*, also seem to have two paralogs of DLP. **Figure 2.** shows a phylogenetic tree of various kinetoplastid TbDLP homologs, in addition to TbDLP homologs in common model organisms such as yeast and frogs. Interestingly, the two *T. evansi* DLP paralogs we identified seem to group with the TbDLP paralogs. The rest of the tree grouped as expected, with *C. fasciculata* and *Leishmania* grouping closely together, and the other non-kinetoplastid models grouping together.

```
#
#
#  Percent Identity  Matrix - created by Clustal2.1
#
#
```

1: TtheDRP	100.00	36.83	34.97	34.27	34.36	34.36	33.97	34.16	36.22	35.13	35.35	35.27	35.42	35.27	35.42	33.98	39.63	38.73	38.31	38.10	38.48
2: PconDLP	36.83	100.00	72.95	72.23	73.14	73.14	74.09	73.79	66.72	73.16	70.50	70.61	70.45	71.23	71.38	38.98	40.71	40.66	42.81	41.78	42.54
3: LmexDLP	34.97	72.95	100.00	90.59	92.91	93.05	83.26	83.26	64.77	70.76	66.97	67.69	67.53	68.45	68.30	36.89	38.40	38.75	39.26	38.78	39.66
4: LmajDLP	34.27	72.23	90.59	100.00	94.25	94.40	84.55	85.13	65.28	71.30	66.92	67.99	67.84	68.29	68.14	36.32	38.32	38.51	39.48	39.00	39.41
5: LdonDLP	34.36	73.14	92.91	94.25	100.00	99.86	84.78	84.78	65.13	71.14	66.16	67.68	67.38	68.14	67.99	36.11	38.39	38.76	39.39	38.76	39.48
6: LinfDLP	34.36	73.14	93.05	94.40	99.86	100.00	84.78	84.78	65.13	71.14	66.16	67.68	67.38	68.14	67.99	36.11	38.24	38.76	39.39	38.76	39.48
7: CfDLP00	33.97	74.09	83.26	84.55	84.78	84.78	100.00	90.97	66.77	73.31	67.57	69.65	69.20	69.80	69.65	36.60	38.71	38.86	38.74	38.08	39.91
8: LpyrDLP	34.16	73.79	83.26	85.13	84.78	84.78	90.97	100.00	65.85	71.78	67.57	68.44	68.44	68.74	68.89	36.36	39.31	38.00	38.90	38.59	39.75
9: TvivDLP	36.22	66.72	64.77	65.28	65.13	65.13	66.77	65.85	100.00	71.89	72.20	72.77	72.46	72.62	72.62	38.94	39.81	40.89	40.51	40.83	40.99
10: TcruDLP	35.13	73.16	70.76	71.30	71.14	71.14	73.31	71.78	71.89	100.00	72.43	73.23	72.92	73.69	73.54	38.79	41.01	40.86	41.31	41.56	41.47
11: TconDLP	35.35	70.50	66.97	66.92	66.16	66.16	67.57	67.57	72.20	72.43	100.00	83.64	83.94	84.24	84.39	38.40	40.62	39.40	39.78	38.94	39.38
12: 20TbDLP	35.27	70.61	67.69	67.99	67.68	67.68	69.65	68.44	72.77	73.23	83.64	100.00	99.55	97.12	97.27	37.96	40.87	40.54	40.94	40.47	41.32
13: 00TeDLP	35.42	70.45	67.53	67.84	67.38	67.38	69.20	68.44	72.46	72.92	83.94	99.55	100.00	97.27	97.73	37.81	40.87	40.38	41.10	40.63	41.64
14: 60TbDLP	35.27	71.23	68.45	68.29	68.14	68.14	69.80	68.74	72.62	73.69	84.24	97.12	97.27	100.00	99.55	38.12	41.19	40.38	40.94	40.63	41.64
15: 40TeDLP	35.42	71.38	68.30	68.14	67.99	67.99	69.65	68.89	72.62	73.54	84.39	97.27	97.73	99.55	100.00	37.96	41.34	40.38	41.10	40.79	41.80
16: DmelDLP	33.98	38.98	36.89	36.32	36.11	36.11	36.60	36.36	38.94	38.79	38.40	37.96	37.81	38.12	37.96	100.00	41.16	40.00	40.33	39.20	40.46
17: ScDnm10	39.63	40.71	38.40	38.32	38.39	38.24	38.71	39.31	39.81	41.01	40.62	40.87	40.87	41.19	41.34	41.16	100.00	46.18	48.32	46.89	48.68
18: CeleDLP	38.73	40.66	38.75	38.51	38.76	38.76	38.86	38.00	40.89	40.86	39.40	40.54	40.38	40.38	40.38	40.00	46.18	100.00	63.30	61.86	64.71
19: XlaeDLP	38.31	42.81	39.26	39.48	39.39	39.39	38.74	38.90	40.51	41.31	39.78	40.94	41.10	40.94	41.10	40.33	48.32	63.30	100.00	88.11	87.17
20: HsapDLP	38.10	41.78	38.78	39.00	38.76	38.76	38.08	38.59	40.83	41.56	38.94	40.47	40.63	40.63	40.79	39.20	46.89	61.86	88.11	100.00	90.74
21: DrerDLP	38.48	42.54	39.66	39.41	39.48	39.48	39.91	39.75	40.99	41.47	39.38	41.32	41.64	41.64	41.80	40.46	48.68	64.71	87.17	90.74	100.00

Figure 3. Percent Identity Matrix of DLP Homologs

Percent identity matrix of Clustal Omega alignment of DLP homologs in kinetoplastids and common model organisms. As expected, kinetoplastids share higher percent identity than more diverged organisms.

Figure 3. shows the percent identity matrix of the Clustal Omega alignment of these kinetoplastid and non-kinetoplastid DLP homologs. As expected, the kinetoplastid homologs share more identity than with non-kinetoplastids. We also used PhyML to create another tree with 100 bootstrap replicates. **Figure 4.** shows the PhyML tree, which is very similar to the Clustal tree. All *Trypanosoma* group identically in

both trees. *Crithidia, Leishmania* and *Leptomonas* group together similarly. There are few differences in the grouping of non-kinetoplastid organisms, but overall, they grouped similarly as well. For example, *S. cerevisiae* and *T. thermophila* grouped together in both trees.

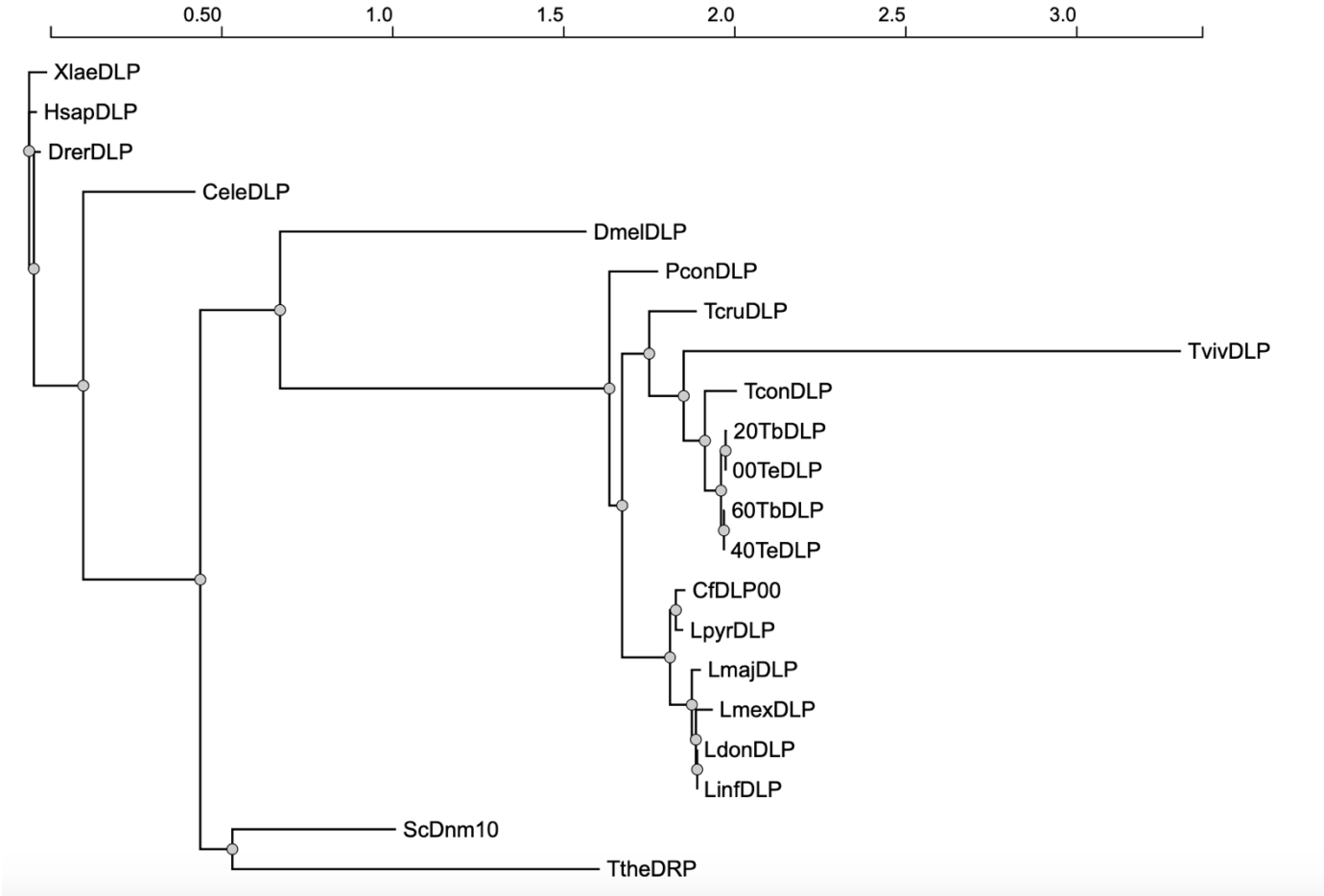

Figure 4. PhyML Phylogenetic Tree of DLP Homologs

Phylogenetic tree from PhyML of DLP homologs in kinetoplastid organisms and common model organisms. 100 bootstrap replicates were used. Again, as in the Clustal Omega tree, the *T. evansi* paralogs group with the *T. brucei* paralogs.

T. brucei has a complex life cycle, alternating between its insect and mammalian hosts. Unlike many unicellular parasites it is always extracellular, and therefore must adapt to the drastically different nutrient environments of the tsetse fly midgut, proventriculus, and salivary gland as well as the bloodstream, adipose, and skin of the mammal (Gibson & Bailey, 2003). In particular, the differences in mitochondrial metabolism between the procyclic form (PCF), that replicates in the tsetse midgut, and the

bloodstream form (BSF), that replicates in the mammalian bloodstream, have been well described. PCF metabolize amino acids, synthesize ATP by oxidative phosphorylation, and have an active, highly branched mitochondrion with numerous cristae. BSF cells are primarily glycolytic, and have a single-straight tubular mitochondrion with no cristae. Little is known about proteins that mediate differentiation between these two mitochondrial states.

On explanation for the existence of multiple DLPs in *T. brucei* is that the two paralogs are needed to mediate the complex mitochondrial remodeling that occurs between life cycle stages. Our new finding of TeDLP paralogs challenges this explanation. *T. evansi* is almost exclusively morphologically represented as thin trypomastigotes, comparable to the *T. brucei* slender and intermediate forms (Misra et al., 2016). Since *T. evansi* spend most of their life in slender and intermediate forms, presumably they would have less complex mitochondrial remodeling. This suggests that both TbDLP and TeDLP paralogs may exist for another, unknown, reason.

Functional analysis of *T. brucei* DLPs is complicated by a possible dual role in endocytosis. *C. fasciculata*, like all other kinetoplastids, have only one predicted DLP. Furthermore, they are monoxenous parasite, and only infect one host, the mosquito. Although they can differentiate between adherent and swimming forms, differences in mitochondrial shape or metabolism between these forms has not yet been described. Therefore, addressing the function of DLP in *C. fasciculata* may shed light on the ancestral role of DLPs in kinetoplastid parasites, and how this may have been expanded in order to fulfill the unique developmental needs of *T. brucei*.

Chapter 4

DLP RNAi and Overexpression in *T. brucei*

DLP has been previously studied in *T. brucei*. We wanted to see what the published phenotypes looked like in our cell lines. We were also hoping to establish this cell line for a control in a large-scale RNAi screen that we plan to do in the future. Andre Schneider gifted us

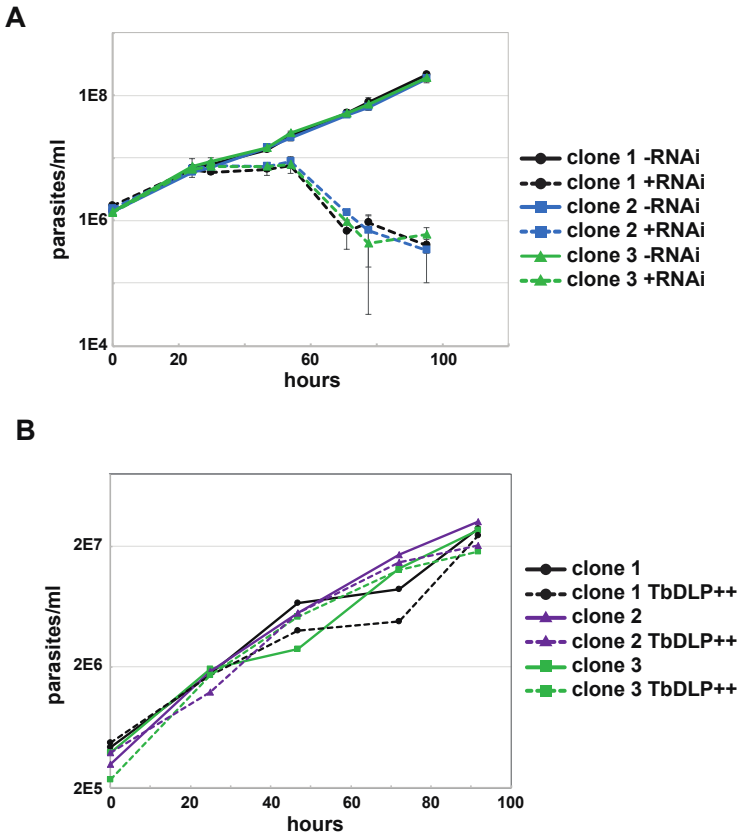

Figure 5. Growth curves of DLP RNAi and overexpression

RNAi and overexpression of DLP in T. brucei. A. Growth curve of DLP knockdown by RNAi. -RNAi cells grew at a steady rate from midlog to stationary phase, while +RNAi clones initially grew, but stopped at around 60 hr. B. Growth curve of cells during overexpression of DLP. All of the cells grew at comparable rates.

the pALC15 DLP RNAi plasmid and the pALC21 DLP overexpression plasmid. We transfected both into our *T. brucei* cell line. After we let each transfection recover, we induced RNAi and

overexpression with tetracycline and counted the cultures to look for a growth phenotype. As seen in **Figure 5.** The +RNAi cells stopped growing at around 60 hours after the addition of tetracycline. The control, -RNAi cells, continued to grow at a normal rate. Both the induced and control DLP overexpression cells grew normally.

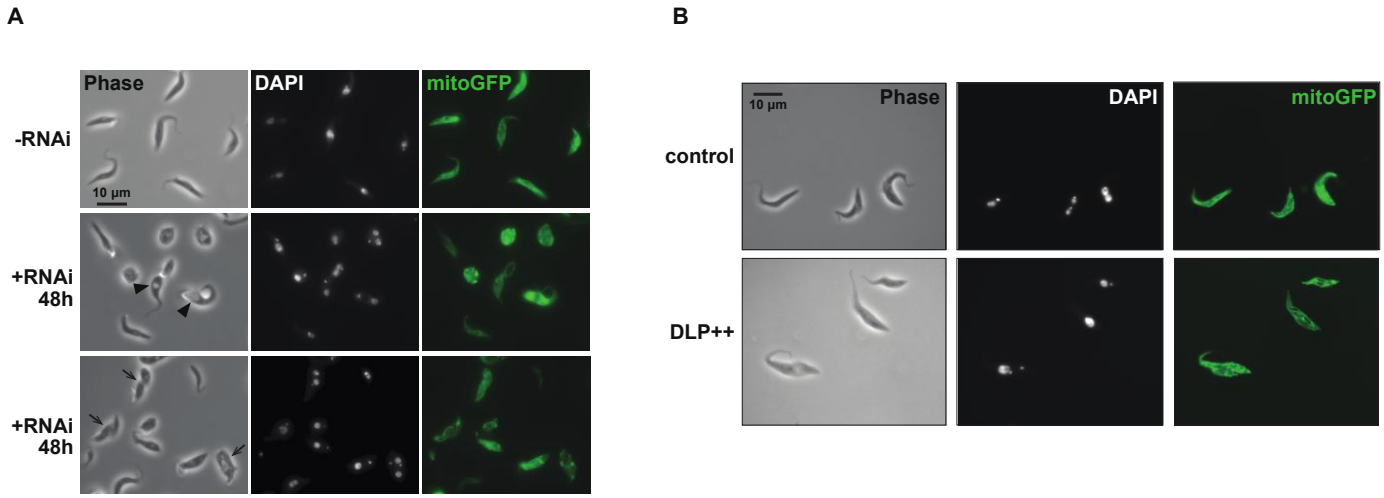

Figure 6. DLP RNAi and overexpression microscopy

A. Fluorescent microscopy of cells following 48 hr of RNAi knockdown of TbDLP. Arrowheads indicate enlarged flagellar pockets indicative of an endocytosis defect. Arrows show cells arrested in cytokinesis. B. Microscopy of cells after 48 hr of TbDLP overexpression. No phenotypes were observed.

We also looked at induced DLP RNAi microscopy. We saw similar phenotypes to those published. After 48 hours of inducing RNAi of DLP we saw the characteristic “big eye” phenotype, which can be seen in **Figure 6 A. panel 2.** All exo- and endocytosis occurs at the flagellar pocket, so when these processes are interrupted, it results in swelling of the pocket, which looks like an eye. This big eye phenotype is indicative of an endocytosis defect, which had previously been published on. We also saw cells arrested in cytokinesis, as shown in **Figure 6 A. panel 3**. We believe that this could be due to the mitochondria not being able to divide, which resulted in cells that could not divide. It has been published that DLP is involved in

mitochondrial division, which this phenotype seems to support. The DLP overexpression microscopy is shown in **Figure 6 B.** We did not see any phenotypes.

Chapter 5

Crithidia Genetic Approaches

Crithidia fasciculata is a model kinetoplastid that is particularly useful in biochemical experiments because it can reach high densities. When the first kinetoplastid genomes were sequenced, pathogenic species were given priority, leading to the development of an array of

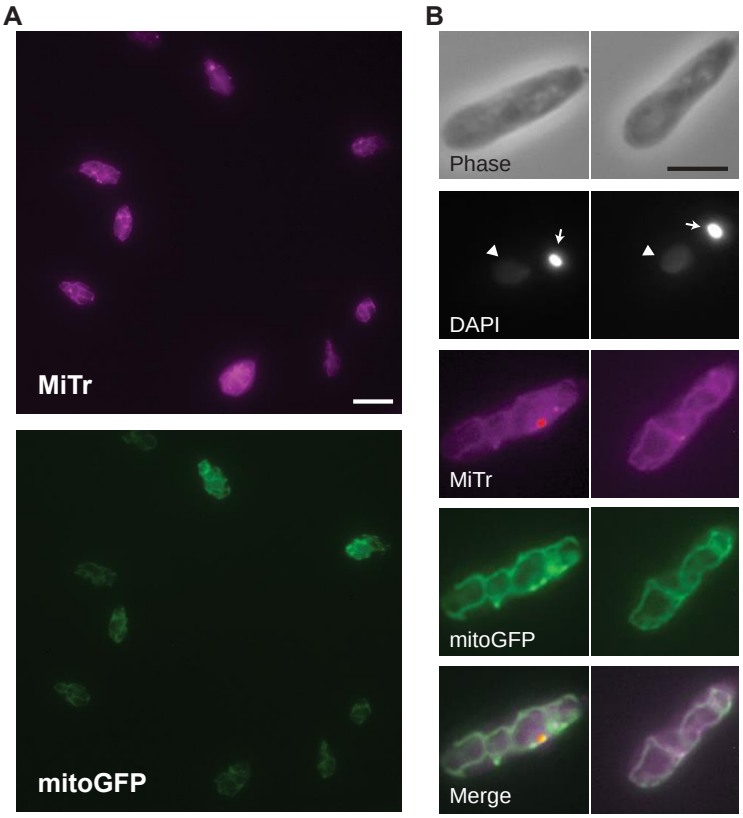

Figure 7. Colocalization of Mitotracker and mitoGFP
We colocalized the mitochondrial stain, Mitotracker, with our *Crtihidia* mitoGFP cell line. A. MitoGFP cells stained with Mitotracker. B. Cells in phase, DAPI stained, Mitotracker (MiTr), mitoGFP, and a merge of both MiTr and mitoGFP. Arrows point to the kinetoplast, arrowheads

genetic tools in these organisms. Now, with the sequencing of the C. fasciculata genome, we are revisiting this organism as a model for kinetoplastid biology. C. fasciculata maintains episomal plasmids, which we have used to create cell lines that express cytoplasmic and mitochondrial GFP. **Figure 7.** shows colocalization of Mitotracker stain with our CfmitoGFP cell line. Mitotracker stains the mitochondria based off of membrane potential. We have also successfully targeted GFP to the tubulin locus by assembling a plasmid using a one-step, 4-way ligation protocol which was developed by the Yates lab for use in Leishmania. We have also used this procedure to make constructs for gene knockout and protein destabilization. Introduction of these constructs into *C. fasciculata* has been challenging. Therefore, we have used a plasmid developed in the Gluenz lab to create a *C. fasciculata* cell line that expresses Cas9 and T7. We are now targeting genes for tagging or knockout using CRISPR/Cas9-mediated cleavage. By using this technique, we hope to allow for a more high-throughput analysis of gene function in *C. fasciculata.*

4-Way Ligation and Destabilizing Domains

The role of TbDLP has not been unambiguously described in the literature, with proposed roles in endocytosis, mitochondrial shape, mitochondrial fission, and cell cycle progression. Analysis of TbDLP function is further complicated by the presence of two nearly identical paralogs that have overlapping but distinct function. For this reason, we decided to investigate the function of DLP in a related kinetoplastid, *C. fasciculata.* These organisms, like all kinetoplastids, with the exception of *T. brucei* and *T. evansi,* have only one predicted DLP. Since DLP knockdown phenotypes are not currently agreed upon, we decided to also knockdown clathrin (CfCLA) as a control. Knockdown of TbCLA in *T. brucei* produces a very well described "big eye" phenotype, in which the flagellar pocket swells. Based on studies in *T. brucei,* we expect that both CfCLA and CfDLP will be essential for growth. Therefore, in order to study the role of these proteins in *C. fasciculata,* for which inducible RNA interference has not yet been established, we decided to express proteins fused with a destabilizing domain using a construct developed for *Leishmania* parasites by Phillip Yates. A destabilizing domain would allow the protein to be stable in the presence of a ligand, but once the ligand was removed, would result in destabilization or knockdown of the protein.

Kinetoplastids are diploid organisms, so any knockout approach will have to target both alleles. In this approach, we could first replace one allele of the gene of interest with a drug resistance marker using homologous recombination. This construct would contain a drug resistance cassette flanked by sequences homologous to regions upstream and downstream of the targeted gene's coding sequence (targeting sequences, TS). Once we confirmed knockout of the first allele, we could transfect in another construct that would fuse a destabilizing domain onto the N-terminus of the other allele. This construct would also contain the upstream and downstream TSs as well as the destabilizing domain cassette and a drug resistance gene. To create these constructs in a single cloning step, we followed Yates' protocol, which uses a 4-way

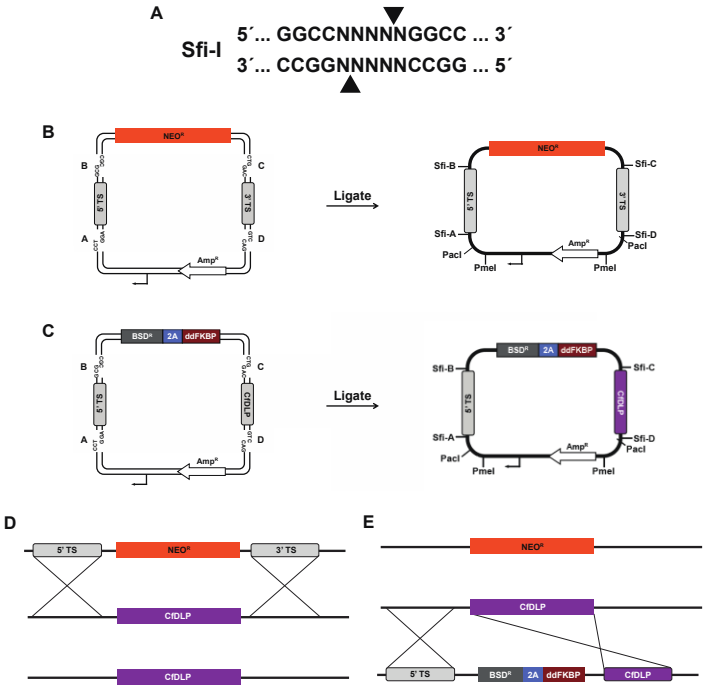

Figure 8. Constructs for inducible knockdown of CfDLP

4-way ligation to build construct for inducible knockdown of CfDLP. **A.** Sequence of Sfi-I restriction sites to create specific ends for 4-way ligation. **B.** Ligation of plasmid backbone, 5' and 3' targeting sequences (TS), and drug resistance cassette, in this case neomycin, in order to replace one allele of CfDLP. **C.** Ligation of destabilizing domain to N-terminus of CfDLP, 5' TS and plasmid backbone to destablize the other allele of CfDLP. **D.** Knockout of one allele of CfDLP with neomycin resistance followed by **E.** fusion of the destabilizaing domain onto the N-terminus of the second allele of CfDLP.

ligation to assemble the pieces of each construct needed to either knockout a gene or fuse a destabilizing domain to the N-terminus. We first made the constructs to target the CfDLP locus.

Since *C. fasciculata* are diploid, we planned to knock out DLP on one allele, and fuse a destabilizing domain to DLP on the other allele. **Figure 8. A** shows the sequence of Sfi-I restriction sites that were used in this 4-way ligation strategy. Sfi-I recognizes sequences with guanine and cytosine repeats flanking any 5 nucleotides repeats, as shown in **Figure 8. B.** This allows restriction sites to be easily added, in addition to creating specific single strand overhangs, which prevent the fragments from ligating in the wrong orientation. We added these sites to upstream of CfDLP, downstream of CfDLP, and the drug cassette, which was neomycin in this case. The pBB backbone was gifted to us from the Yates lab, and already had Sfi-I sites. **Figure 8. B** shows the 4 fragments that were fused together to make a plasmid that could replace CfDLP with neomycin resistance. Using a similar approach, we created a construct that would replace one allele of CfCLA with neomycin resistance.

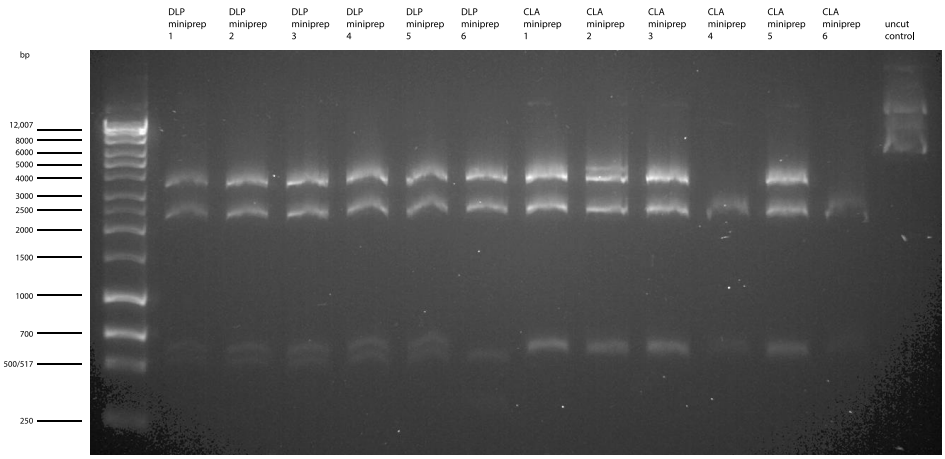

Figure 9. Diagnostic digest of DLP and CLA knockout constructs

Diagnostic digest of DLP and CLA neomycin knockout construct minipreps cut with Sfi-I. Expected bands for DLP minipreps at 2165 bp, 3224 bp, 523 bp, and 596 bp. Expected bands for CLA minipreps at 3224 bp, 2165 bp, and 570 bp.

We confirmed the 4-way ligation products through diagnostic digests, with Sfi-I, of the miniprepped transformation products. As seen in **Fig 9.,** 4 distinct bands are visible for DLP minipreps 1-5. In the case of CLA minipreps 1-3 and 5 only 3 bands are visible, since the TS fragments for both upstream and downstream of CfCLA were expected to be ~570 bp. The approximately 570 bp band in CLA minipreps 1-3 and 5 appears slightly brighter than the other bands, indicating that there was twice as much DNA. We sent DLP miniprep 3, DLP miniprep 4, CLA miniprep 1, and CLA miniprep 3 for sequencing. Sequencing of DLP minipreps confirmed that the 4-way ligation was a success. The sequencing for the CLA minipreps revealed a few positions in the upstream and downstream TSs that differed from the genome. This suggests either the presence of single nucleotide polymorphisms (SNPs) or the presence of multiple alleles for these loci. This may make homologous recombination difficult, for instance if a construct had an upstream TS from allele 1 of a locus and a downstream TS corresponding to allele 2. Due to discrepancies in the CLA sequences we decided to continue pursuing DLP, and move away from creating CLA knockout constructs.

After making the construct to knock out DLP on one allele, we again used Yates' 4-way ligation protocol to ligate the pBB backbone, 5' targeting sequence upstream of DLP, the entire DLP gene, and the destabilizing domain ddFKBP. **Figure 8. C** shows the ligation of these 4 constructs to make a plasmid that has an N-terminal destabilizing domain fused to *C. fasciculata* DLP. **Fig 8. D** depicts homologous recombination of the neomycin resistance in place of CfDLP on one of the alleles. Homologous recombination of the N-terminal destabilizing domain fusion protein on the other allele can be seen in **Fig 8. E**.

CRISPR/Cas9

A CRISPR/Cas9 *C. fasciculata* cell line would improve the efficiency of homologous recombination, while at the same time allowing the use of smaller homology flanks, which could be made in a single PCR step instead of cloning. Beneke et al. published their work on creating CRISPR/Cas9 cell lines in *Leishmania major, Leishmania mexicana, and Trypanosoma brucei.* Since *C. fasciculata* are closely related to *Leishmania,* we used Beneke et al.'s method to create a *C. fasciculata* CRISPR/Cas9 cell line.

Beneke et al. made the pTb007 plasmid, which has FLAG-tagged Cas9, T7 RNA polymerase, and hygromycin resistance inserted between the 3'UTR and 5'UTR of *L. major* β-tubulin, as shown in **Figure 10. A.** This construct was used to integrate the Cas9/T7/Hyg cassette in between two beta-tubulin genes.

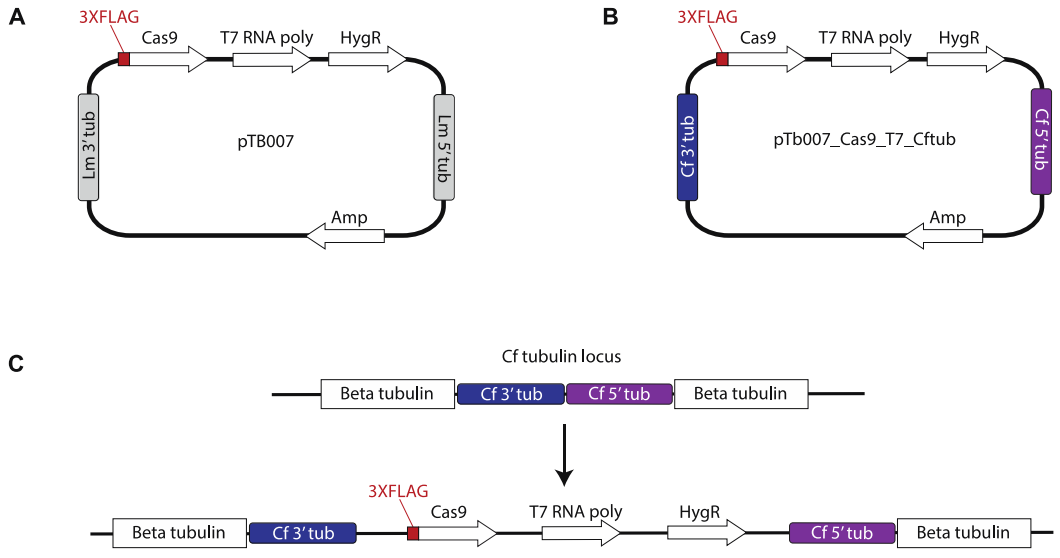

Figure 10. pTb007 cloning strategy

A tool for CRISPR/Cas9 genome editing in C. fasciculata. A. pTB007 plasmid from Gluenz lab developed to integrate Cas9/T7 into the Leishmania genome. B. CRISPR/Cas9 plasmid modified with fragments targeting the Crithidia tubulin locus. C. Integration of the Cas9/T7 polymerase construct into the *C. fasciculata* tubulin locus.

We wanted to create a construct that would introduce a GFP gene in between an alpha-tubulin and a beta-tubulin gene. This locus is a useful place for the integration of constructs since it probably is transcribed in all life cycle stages. The tubulin array has also been used in *T. brucei* as a target for integration of various constructs needed for tetracycline-inducible RNAi. Another advantage of integrated constructs is that one can select for clonal cell lines and achieve homogenous expression across the entire cell population. Genes in episomal constructs, such as the one used to create our mitoGFP line, are maintained at different levels in different cells, leading to heterogenous expression. In the future, if we wanted to create an integrated mitoGFP line, we could insert a mitoGFP construct into the tubulin locus, producing a line in which each cell has a strong mitoGFP signal. This line would improve our analysis of mitochondrial shape across the cell population for cells in different stages of the cell cycle.

In order to show that we could target a similar locus in integrate into the *Crithidia* genome, we had to replace the *Leishmania* tubulin 3'UTR and 5'UTR with corresponding fragments from the *Crithidia* tubulin intergenic region. **Figure 10. B** shows the pTb007 plasmid, that has Cas9, T7 polymerase, and hygromycin resistance, with *Crithidia* tubulin UTR's cloned in. The predicted integration of Cas9 and T7 polymerase with hygromycin resistance into the tubulin locus of *C. fasciculata* is shown in **Figure 10. C.**

In order to integrate the *Leishmania* Btub construct into *C. fasciculata*, we first had to replace the *Leishmania* processing signals with *Crithidia* processing signals. To create our GFP-tubulin targeting construct, we needed to assemble ~500 bp of the region downstream of the beta tubulin gene, the GFP gene, ~500 bp of the region upstream of the alpha tubulin gene, and the plasmid backbone. We used Yates 4-way ligation protocol to achieve this in a single step, creating pNUSBtubGFPHygcH. After ligating, we transformed the constructs and ran Sfi-I diagnostic digests of minipreps to find the right construct. **Figure 11.** shows the results of the digest. Minipreps 4 and 6 both had 4 bands, which appeared to be the expected sizes. We also confirmed the identity of minipreps 4 and 6 with sequencing.

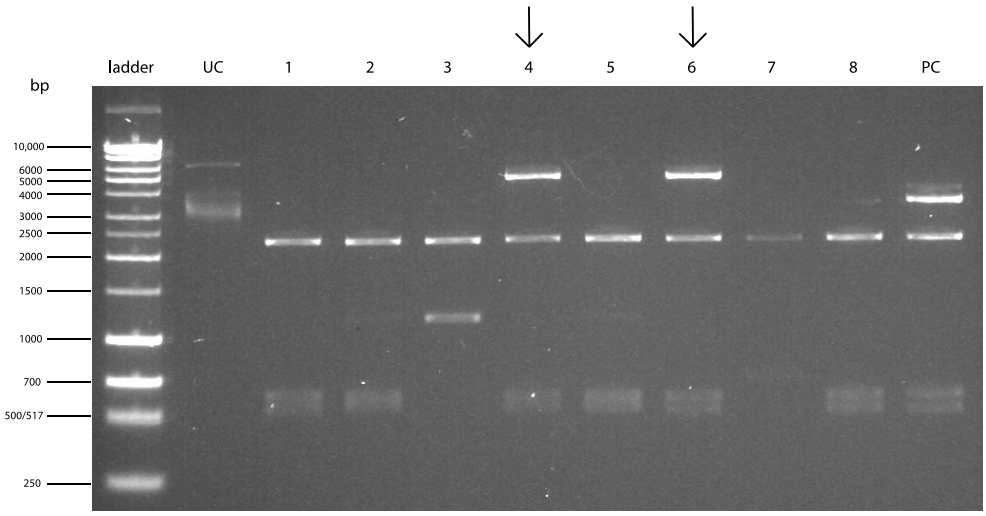

Figure 11. Diagnostic digest of pNUSBtubGFPHygcH miniprep constructs with Sfi-I

We picked 8 colonies from pNUSBtubGFPHygcH transformations to grow up and miniprep. Minipreps were cut with Sfi-I with 4 expected products of sizes ~4545 bp, ~2100 bp, ~570 bp, and ~510 bp. "UC" shows the uncut control, and lane 11 shows a positive control of a DLP knockout construct that was also made with the 4-way ligation method. Minipreps 4 and 6, designated with arrows, appear to have all 4 bands of the expected sizes.

We linearized pNUSBtubGFPHygcH midiprep 6 with PmeI, transfected it into our CfC1 cell line, and selected using hygromycin. After cells recovered from selection, we imaged them with fluorescent microscopy. CfBtubGFP cells expressed a uniform cytoplasmic GFP signal, indicating that we successfully integrated GFP into the tubulin locus of *Crithidia.* Fluorescent microscopy can be seen in **Figure 12.** We used CfC1 parental cells as a control. At an exposure of 4045 ms, the CfC1 cells show

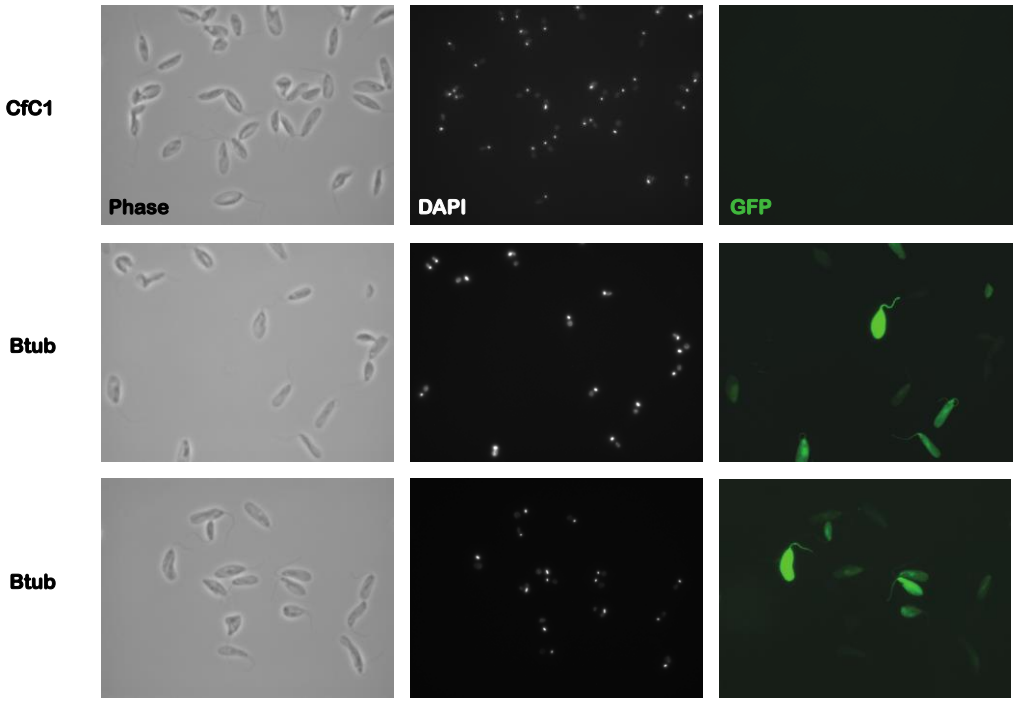

Figure 12. CfpNUSBtubGFPHygcH microscopy

Microscopy of CfpNUSBtubGFPHygcH (Btub) with CfC1 cell line as a control. CfC1 cells expressed some autofluorescence at 4045 ms exposure. The Btub cells were imaged with exposure times of 625 ms and 1544 ms, respectively. Some cells were expressing higher levels of GFP than others. Btub cells were expressing GFP cytoplasmically, while CfC1 control cells did not have any cytoplasmic signal.

some autofluorescence, which is primarily mitochondrial and has been previously observed. The GFP signal in CfBtubGFP cells is much stronger, allowing for shorter exposure times, and is clearly present in the cytoplasm. Since this GFP gene is stably integrated, it is expected that all cells will have the same level of GFP expression. While all cells expressed some level of GFP, as seen in **Figure 12.,** some cells had higher levels of GFP expression than others. Phase imaging showed that the shape and size of CfBtubGFP cells were comparable to the control. DAPI images showed that the kinetoplast and nucleus also appeared normal in CfBtubGFP cells. In order to definitively confirm that we have targeted tubulin in every cell, we will also perform linking PCR. In addition, we will clone out CfBtubGFP cells and screen for clones with homogenous GFP expression. One possible explanation for the heterogenous

expression of GFP in the CfBtubGFP cells is that the PmeI digest to linearize the pNUSBtubGFPHygcH plasmid was not complete, and that some of the trasnfectants are expressing the construct as an episome. If this happened, the integrated transfectants should be able to be found by screening clones for homogenous GFP expression. Another possible explanation is that GFP expression is somehow coordinated with the cell cycle. CfBtubGFP cells are currently being cloned and screened for homogenous GFP expression.

While we were creating the CfBtubGFP cell line, and the CftubCas9T7Hyg construct for integration, we decided to transfect the *Leishmania* pTb007 construct into our CfC1 cell line to see if it could be expressed as an episome. Although this construct has *Leishmania* tubulin sequences for integration, the construct is based on the pNUS plasmid, meaning that the Cas9/T7/Hyg cassette has upstream and downstream processing signals that are derived from *C. fasciculata.* We purified the pTb007 construct, transfected it into CfC1 wild-type cells and selected for presence of the plasmid with hygromycin. After recovery, we confirmed the expression of Cas9 by making whole cell lysates, running them on an SDS-PAGE gel, and analyzing in a Western blot probed with anti-FLAG, as shown in **Figure 13.** Only the CfpTb007 cell line had a band at ~165kDa, which was the expected size of hSpCas9FLAG. There was a non-specific band at ~50 kDa that was present in both the control and CfpTb007. The Coomassie stained gel showed that the loading was comparable, with the CfpTb007 lysate containing slightly more protein.

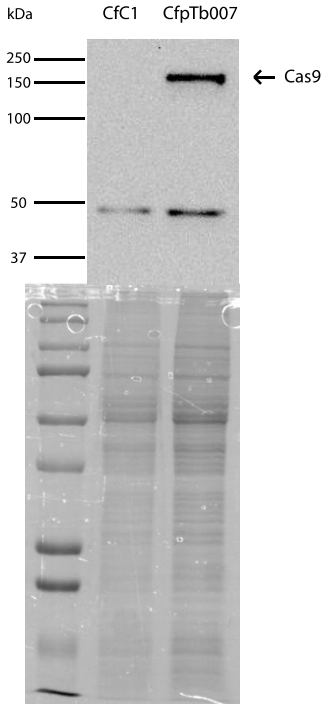

Figure 13. pTb007 Western blot

Upper panel: Whole cell lysates of CfC1 wildtype and CfpTb007 cell lines were analyzed in a Western blot probed with anti-FLAG. Arrow points to expected band at ~165kDa, which is the calculated size of hSpCas9FLAG. Off target binding at ~48 kDa is in both the control and CfpTb007. Lower panel: Coomassie stained gel.

Once we confirmed that Cas9 was being constitutively expressed as an episome in our CfpTb007 cell line, we chose a gene to knockdown using CRISPR/Cas9 mediated cleavage. Beneke et al. were able to knock out *pf16* (paralyzed flagella protein 16 LmxM.20.1400) in *L. mexicana. Pf16* is part of the central axoneme of the flagellum, and genetic knockout of the *pf16* gene resulted in immotile cells, an easily identifiable phenotype. Since we are following Beneke et al.'s method for CRISPR/Cas9 genome modification, and since *Leishmania* species are closely related to *C. fasciculata*, we decided that *pf16* would be a good choice for the first gene to knockout in our CfpTb007 line. We targeted the *C. fasciculata* homolog of *pf16* (CFAC1_170028000), which is annotated as a putative axoneme central

apparatus protein. We wanted to use the CfPF16 knockout as a proof of principle, to show that we could use CRISPR/Cas9-mediated cleavage to replace a gene with a drug resistance cassette.

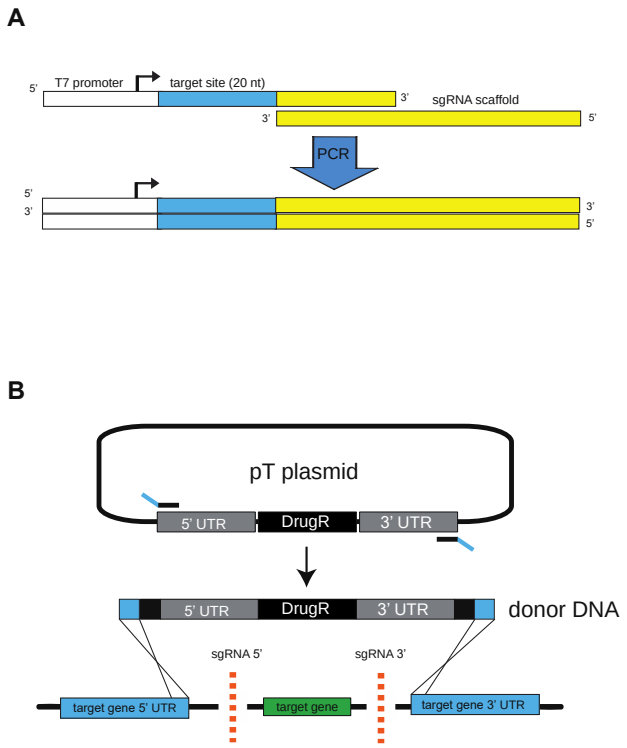

Figure 14. Strategy for designing sgRNA and donor cassette

A. Fusion PCR strategy to create single-guide RNA (sgRNA) for use in CRISPR/Cas9 cells. Specific oligo contains a T7 promoter, 20 nucleotides of the target site, and part of the sgRNA scaffold template provided by the Gluenz lab. The resulting sgRNA template is transfected into C. fasiculata and transcribed in vivo by T7 RNA polymerase. For gene knockout, two sgRNA templates would be created, with target site specificity up and downstream of the target gene. B. Strategy for PCR generation of donor DNA cassettes from the pT plasmid to be transfected along with the appropriate sgRNA templates to direct Cas9-mediated cleavage and knockout of the target gene.

In the Beneke et al. system, guide RNA (sgRNA) templates are created by PCR and then transfected into Cas9-expressing cells along with the donor cassettes. The guide RNA templates contain a T7 promoter so that they can be transcribed in vivo by the T7 polymerase. **Figure 14. A** shows the strategy for designing the sgRNA's. We used a fusion PCF reaction to create sgRNAs containing an sgRNA scaffold template (provided by the Gluenz lab), the T7 binding site, and 20 nucleotides of the target site ending in a PAM sequence, which was identified by The Eukaryotic Pathogen CRISPR guide

RNA/DNA Design Tool (http://grna.ctegd.uga.edu). The PAM was not included in the final sgRNA. For gene knockout, we targeted sites upstream and downstream from the gene of interest. This would result in 2 double stranded cuts, which would greatly increase the likelihood of homologous recombination at these sites.

One of the benefits of CRISPR/Cas9 mediated cleavage is that it makes homologous recombination much more efficient. This allows us to use smaller homology flanks when designing the donor DNA cassettes that will replace our targeted genes. In *Leishmania,* 30 nucleotides of homology was sufficient for homologous recombination in the presence of a Cas9-induced DNA break. Therefore, homology flanks (HFs) can be added onto the DNA primers that are used to amplify drug cassettes, thereby creating the donor DNAs by PCR. **Figure 14. B** shows the strategy for designing the donor cassettes to replace the gene of interest. The donor cassettes contain 30 nucleotides of homology to

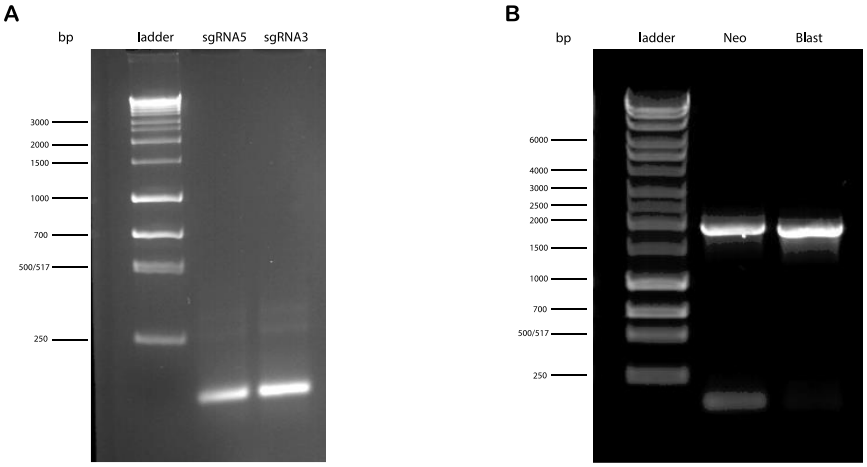

Figure 15. PCR amplification of sgRNA and donor cassettes for PF16 knockout

PCR products of sgRNA and donor cassettes for PF16 knockout run on a 1% agarose gel. **A.** sgRNA PCR products. Expected size ~120 bp. **B.** PCR products for amplification of neomycin resistance (Neo) and blasticidin resistance (Blast) cassettes. Expected size of Neo cassette is ~1807 bp and the expected size of the Blast cassette is ~1773 bp

regions directly adjacent to the sgRNA cut sites. We used this strategy to amplify a blasticidin resistance donor cassette and a neomycin donor cassette. We ran the sgRNA and donor DNA PCR products on a 1% agarose gel to make sure that they were the correct size. **Figure 15. A** shows the 5' and 3' sgRNA

reaction products, which are the expected size of ~120 bp. **Figure 15. B** shows the drug resistance donor cassette PCR reactions. The neomycin resistance donor reaction product was the expected size of ~1807 bp, and the blasticidin donor reaction product was the expected size of ~1773 bp. We transfected the sgRNA's and donor cassettes into the CfpTb007 cell line, selected with neomycin and blasticidin, and are waiting for transfectants to recover.

Chapter 6

Discussion

Our bioinformatic analysis of DLP in kinetoplastids did not reveal any new insights into the functional role of the protein. However, we were able to identify paralogs in *Trypanosoma evansi* that were not previously discussed in the literature. Interestingly, each of these two *T. evansi* DLP paralogs grouped more closely with one or the other *T. brucei* DLP paralogs. This indicates that the event that led to two DLP paralogs may have occurred before *T. brucei* and *T. evansi* diverged. The literature previously stated that *T. brucei* is the only subclade to have two paralogs of DLP. This bioinformatic analysis suggests that *T. evansi* also has two paralogs of DLP. More work needs to be done to characterize these two paralogs. It would be interesting to see if the *T. evansi* paralogs also have distinct but overlapping roles, as is the case with the two TbDLP paralogs.

We were able to confirm some of the published phenotypes for TbDLP in our *T. brucei* mitoGFP-expressing cell lines. Using the published constructs for TbDLP knockdown by RNAi and overexpression (Chanez et al.), we sought to validate the use of our mitoGFP-expressing *T. brucei* line for evaluation of mitochondrial phenotypes. RNAi-mediated knockdown of TbDLP in our TbPCFmitoGFPE10 line produced cells with a “big eye” phenotype, consistent with disruption of endocytosis, and a cell cycle defect. There was a growth phenotype at around 60 hours post induction of RNAi. The overexpression mutants had no observed growth phenotype or mitochondrial phenotypes. Both of these results are consistent with what has been published (Chanez et al, 2006). We observed many DLP RNAi cells that were arrested in cytokinesis. Chanez et al. suggested that if the mitochondrion was not able to divide, the cell would not be able to divide, indicating a novel check point for mitochondrial division. Our data supports this finding. Our results indicate that our mitoGFP-expressing cell line can be used to study the

effects of RNAi-mediated knockdown, and will be used for a large-scale RNAi screen we are planning to do in the future.

Since the knockdown phenotype for TbDLP is complicated by the fact that there are two paralogs with distinct but overlapping functions, along with its dual functionality in endocytosis and mitochondrial fission, we decided to try to knock down DLP in *C. fasciculata*. The *C. fasciculata* genome predicts only one DLP gene, which is more typical for kinetoplastids. In addition, no one has yet demonstrated changes in mitochondrial shape during the life cycle of *C. fasciculata*, which is a well-studied phenomenon in *T. brucei*. We hypothesized that knocking down the single DLP gene in *C. fasciculata* might provide some clarity as to the ancestral function of this protein in kinetoplastids. RNAi has yet to be established in *C. fasciculata*, so we first tried a genetic knockout using homologous recombination. Kinetoplastids are diploid organisms, so we designed two constructs. The first construct would replace one copy of CfDLP with a neomycin resistance gene. As expected, after sequential introduction of these constructs, we were not able to obtain cells that were resistant to both drugs, which supports our theory that DLP is an essential gene. To get around this, we created a construct that would fuse a destabilizing domain to DLP on one allele, which we could introduce into a cell line in which the other DLP allele had been knocked out. We were able to confirm that we had made the constructs for the destabilizing domain fused to DLP, but we were not able to successfully transfect both the DLP knockout and destabilizing domain into the same cell line. We believe that this is due to the low efficiency of homologous recombination along with the presence of single nucleotide polymorphisms in the targeting regions. In order to increase the efficiency of homologous recombination we created a CRISPR/Cas9 cell line in *C. fasciculata*.

We first sought to stably integrate this CRISPR/Cas9 construct into the tubulin locus, as had been done in *L. mexicana* (Beneke et al., 2017). To show that we could successfully target this locus, which, to our knowledge, has never been done in *C. fasciculata* before, we created a construct that would integrate GFP into the intergenic region between two tubulin genes. We are still working on confirming this integration event; however, using fluorescent microscopy we showed that the cells had a cytoplasmic

GFP signal. By integrating GFP into the beta tubulin loci, we have shown that it is possible to integrate other constructs into this location. We plan to integrate the CRISPR/Cas9 construct into the beta tubulin loci in the near future. Simultaneously, since *Crithidia* are able to maintain plasmids as episomes, we created a CRISPR/Cas9 episomal cell line. Since there is a FLAG tag on Cas9, we were able to use a Western blot to prove that the CRISPR/Cas9 construct is being constitutively expressed in the cells.

After confirming that we had created a CRISPR/Cas9-competent cell line in *C. fasciculata*, we wanted to choose a gene to knockout that would have an obvious phenotype. We chose *pf16*, a flagellar pocket protein, since the knockout of *pf16* in *Leishmania* resulted in immotile cells, which would be easy to identify. Importantly, *L. mexicana pf16* knockout cells were viable, meaning that we should be able to obtain double-knockout cells. After confirming the size of the sgRNA and donor cassettes with gel electrophoresis, we transfected them into our episomal CRISPR/Cas9 line. Our first attempt did not result in viable cells. We are now troubleshooting this procedure by transfecting more DNA, and using different donor cassettes that contain processing signals derived from *C. fasciculata* rather than *Leishmania.* We are still waiting for transfectants to come up. If this doesn't work, we could also try transfecting constructs with longer homology arms. In *L. mexicana,* 30 nucleotides of homology was shown to be sufficient for homologous recombination in the presence of a Cas9-mediated double stranded break; however, it is possible that *C. fasciculata* will need longer regions of homology. Since we have already made constructs with ~500 nucleotide homology arms to target CfDLP, we could use these as donor cassettes in our CRISPR/Cas9 line to increase the efficiency of their integration.

Chapter 7

Conclusion

Crithidia fasciculata and *Trypanosoma brucei* offer insight into the basal machinery for mitochondrial dynamics in kinetoplastids, as well as eukaryotes as a whole. Investigating the role of proteins, such as DLP, in mediating life cycle and environment-induced changes in mitochondrial shape will provide a clearer picture of the role of mitochondrial dynamics in these organisms, and perhaps provide insights into how other eukaryotes shape their mitochondria. *C. fasciculata* is a useful model kinetoplastid with limited tools for genetic manipulation. The development of a CRISPR/Cas9 cell line in *C. fasciculata* will allow for efficient and effective gene manipulation, which would allow mutant phenotypes to be more easily identified. We have shown that the CRISPR/Cas9 construct is being constitutively expressed as an episome in our *C. fasciculata* cell line. We are continuing to work on integrating the CRISPR/Cas9 construct into the *C. fasciculata* genome. Our future work will also focus on designing single guide RNAs and donor drug cassettes to knock out the protein *pf16*, in addition to fusing a destabilizing domain to DLP for transient, inducible knock down. While these genes are of special interest to our lab, the CRISPR/Cas9 *C. fasciculata* cell line could be used to knock down or tag any number of genes, and will be a useful tool for the genetic manipulation of *C. fasciculata* in future experiments.

BIBLIOGRAPHY

Allen, C. L., Goulding, D., & Field, M. C. (2003). Clathrin-mediated endocytosis is essential in Trypanosoma brucei. *The EMBO Journal*, *22*(19), 4991–5002. https://doi.org/10.1093/emboj/cdg481

Beneke, T., Madden, R., Makin, L., Valli, J., Sunter, J., & Gluenz, E. (2017). A CRISPR Cas9 high-throughput genome editing toolkit for kinetoplastids. *Royal Society Open Science*, *4*(5). https://doi.org/10.1098/rsos.170095

Benz, C., Stříbrná, E., Hashimi, H., & Lukeš, J. (2017). Dynamin-like proteins in Trypanosoma brucei: A division of labour between two paralogs? *PLOS ONE*, *12*(5), e0177200. https://doi.org/10.1371/journal.pone.0177200

Cassidy-Stone, A., Chipuk, J. E., Ingerman, E., Song, C., Yoo, C., Kuwana, T., … Nunnari, J. (2008). Chemical inhibition of the mitochondrial division dynamin reveals its role in Bax/Bak-dependent mitochondrial outer membrane permeabilization. *Developmental Cell*, *14*(2), 193–204. https://doi.org/10.1016/j.devcel.2007.11.019

Chanez, A.-L., Hehl, A. B., Engstler, M., & Schneider, A. (2006). Ablation of the single dynamin of T. brucei blocks mitochondrial fission and endocytosis and leads to a precise cytokinesis arrest. *Journal of Cell Science*, *119*(Pt 14), 2968–2974. https://doi.org/10.1242/jcs.03023

DiMaio, J., Ruthel, G., Cannon, J. J., Malfara, M. F., & Povelones, M. L. (2018). The single mitochondrion of the kinetoplastid parasite Crithidia fasciculata is a dynamic network. *PloS One*, *13*(12), e0202711. https://doi.org/10.1371/journal.pone.0202711

Fulwiler, A. L., Soysa, D. R., Ullman, B., & Yates, P. A. (2011). A rapid, efficient and economical method for generating leishmanial gene targeting constructs. *Molecular and Biochemical Parasitology*, *175*(2), 209–212. https://doi.org/10.1016/j.molbiopara.2010.10.008

García-Salcedo, J. A., Pérez-Morga, D., Gijón, P., Dilbeck, V., Pays, E., & Nolan, D. P. (2004). A differential role for actin during the life cycle of Trypanosoma brucei. *The EMBO Journal*, *23*(4), 780–789. https://doi.org/10.1038/sj.emboj.7600094

Gibson, W., & Bailey, M. (2003). The development of Trypanosoma brucei within the tsetse fly midgut observed using green fluorescent trypanosomes. *Kinetoplastid Biology and Disease*, 13.

Hinshaw, J. E. (2000). Dynamin and Its Role in Membrane Fission. *Annual Review of Cell and Developmental Biology*, *16*(1), 483–519. https://doi.org/10.1146/annurev.cellbio.16.1.483

Lackner, L. L. (2013). Determining the shape and cellular distribution of mitochondria: the integration of multiple activities. *Current Opinion in Cell Biology*, *25*(4), 471–476. https://doi.org/10.1016/j.ceb.2013.02.011

Lai, D.-H., Hashimi, H., Lun, Z.-R., Ayala, F. J., & Lukeš, J. (2008). Adaptations of Trypanosoma brucei to gradual loss of kinetoplast DNA: Trypanosoma equiperdum and Trypanosoma evansi are petite mutants of T. brucei. *Proceedings of the National Academy of Sciences of the United States of America*, *105*(6), 1999–2004. https://doi.org/10.1073/pnas.0711799105

Misra, K. K., Roy, S., & Choudhury, A. (2016). Biology of Trypanosoma (Trypanozoon) evansi in experimental heterologous mammalian hosts. *Journal of Parasitic Diseases: Official Organ of the Indian Society for Parasitology*, *40*(3), 1047–1061. https://doi.org/10.1007/s12639-014-0633-1

Morgan, G. W., Goulding, D., & Field, M. C. (2004). The single dynamin-like protein of Trypanosoma brucei regulates mitochondrial division and is not required for endocytosis. *The Journal of Biological Chemistry*, *279*(11), 10692–10701. https://doi.org/10.1074/jbc.M312178200

Ramachandran, R. (2018). Mitochondrial dynamics: The dynamin superfamily and execution by collusion. *Seminars in Cell & Developmental Biology*, *76*, 201–212. https://doi.org/10.1016/j.semcdb.2017.07.039

Tetaud, E., Lecuix, I., Sheldrake, T., Baltz, T., & Fairlamb, A. H. (2002). A new expression vector for Crithidia fasciculata and Leishmania. *Molecular and Biochemical Parasitology*, *120*(2), 195–204. https://doi.org/10.1016/S0166-6851(02)00002-6

Academic Vita of Madeline Malfara

Email: madelinemalfara@gmail.com

Education
Major(s) and Minor(s): Major: Biology- Vertebrate Physiology Option.
Honors: Completing Honors Thesis in Biology

Thesis Title: Mitochondrial Dynamics in *Crithidia fasciculata* and *Trypanosoma brucei*
Thesis Supervisor: Dr. Megan Povelones

Work Experience:
Undergraduate research
Date: May 2017-present
Title: Undergraduate Research Assistant
Description:
- Investigating *T. brucei* and *C. fasciculata* in Dr. Megan Povelones' lab.
- Completed Phillip Yate's protocol for 4-way ligation to create a tool to study dynamin like protein (DLP) and clathrin through gene knockdown in *C. fasciculata*.
- Transfecting *T. brucei* with gene for overexpression and knockdown of DLP. Successfully transfecting, cloning out, imaging and making growth curves for knockdown.
- Compiling research skills for comprehension, analysis and presentation of primary literature.

Institution/Company (including location): Povelones Lab at Penn State Brandywine
Supervisor's Name: Dr. Megan Povelones

Anexinet Part-Time Social Listening Analyst
Date: Jan 2019-present
Title: Part-Time Social Listening Analyst
Description:
- Analyst for Real Time Monitoring team at Anexinet.
- Monitor live RSS feeds for one of Anexinet's major clients.
- Calculate social media volume for deliverables.
- Assist in writing deliverables to continuously update the client on any recent issues.

Institution/Company (including location): Anexinet, Blue Bell, PA
Supervisor's Name: Jennifer Dandy

Assistant to Laboratory Coordinator
Date: Oct 2015-Dec 2016
Title: Assistant to the Laboratory Coordinator
Description:
- Helped prepare teaching laboratories for courses in Biology, Chemistry, and Physics.
- Developed new laboratory curriculum experiments and trouble shot areas of difficulty.
- Prepared large and small-scale solutions and media for use in laboratory courses.
- Inoculated bacterial cultures for use in laboratory courses.

- Employed good laboratory housekeeping and followed all safety procedures.
- Managed laboratory inventory and submitted order requests to the laboratory coordinator.
- Managed chemical and biological hazardous waste disposal.

Institution/Company (including location): Penn State Brandywine
Supervisor's Name: Amanda Gunlefinger

Lion Ambassador
Date: Oct 2015-present
Title: Vice President of Lion Ambassadors
Description:
- Tour potential applicants to Penn State Brandywine.
- Assist at admissions events on campus.
- Support the admissions department in recruiting and maintaining students on campus.

Institution/Company (including location): Admissions at Penn State Brandywine
Supervisor's Name: Kari Berton

Grants Received:
Schreyer Ambassador Awards:
PAracon Parasitology Conference
Penn State Brandywine Global Program to Barcelona, Spain

Awards:
The Jane E. Cooper Honors Program (2015-current)
Schreyer Honors College (2016-current)
The President's Freshman Award (2016)
The Edward S. J. Tomezsko Scholarship (2016)
1920 Class Scholarship Award (2017)
NCFA Scholar Athlete (2016, 2017, 2018)
PSUAC softball champion (2016, 2017, 2018)
PSUAC Academic All-Conference (2016, 2017, 2018)
USCAA National Academic Team (2017, 2018)
CoSIDA Google Cloud Academic All-District Softball Team (2018)
CoSIDA Google Cloud All-American College Division Softball Second Team (2018)
D'Iorio Family Research Award (2018)
Eric A. and Josephine S. Walker Award for Student Leadership (2018)
STEM Research Award at EURECA 2018
Social Science and Humanities Research Award at EURECA,(2017)
Vairo Library Undergraduate Award for Information Literacy

Publications: DiMaio, J., Ruthel, G., Cannon, J. J., Malfara, M. F., & Povelones, M. L. (2018). The single mitochondrion of the kinetoplastid parasite Crithidia fasciculata is a dynamic network. *PloS One*, *13*(12), e0202711. https://doi.org/10.1371/journal.pone.0202711

Presentations:
Undergraduate Research Poster Contest, December 2017

- Presented "The single mitochondrion of *Crithidia fasciculata* is a dynamic network" with Dr. Megan Povelones and John Dimaio in the undergraduate category of the American Society for Cell Biology-European Molecular Biology Organization Meeting (ASCB-EMBO)

Presented Undergraduate Research, June 2017

- Presented "Studying the transmission of substituent effects on comparable 1H and 13C sites in monosubstituted benzenes and pyridines" at the Middle Atlantic Regional Meeting (MARM) of the American Chemical Society (ACS) with Dr. John Tierney

Community Service Involvement:
-Assistant Coach for Ardsley North Hills Athletic Association (ANHAA) ten-year-old, twelve-year-old and fifteen-year-old softball teams (2014-Current)
-Student leader volunteer for the 2017 and 2018 STEM Options Program for seventh and ninth grade girls.
-Volunteer at Copper Beech Elementary School 5th and 6th grade musical production
-Shadow Dr. Nathan Lent at Family Practice of Willow Grove (2017-present)
-Member of Team Impact Leadership Team
-Pre-med program at Abington-Jefferson Health-2018

International Education (including service-learning abroad):
Global program to Barcelona, Spain in Fall 2016

Language Proficiency: English